

Chapter 5

Periodic Variables and Binary Sequences

5.1 Periodic Variable Stars

The primary purpose of our project is to search for brightness changes resulting from photospheric stellar activity on the stars in the four clusters. However, the data are also well-suited to searching for periodic variables such as eclipsing binaries and pulsating stars. The V filter data for the well-observed stars in Phase I consist of nearly 2000 frames over the six season time frame. The Phase II data were taken through the BVR filters for one to two years, depending on the cluster. Both data sets have their advantages in a search for periodic variability: the Phase I data have a longer time baseline, while the Phase II data have lower noise levels.

I searched the data for periodic variables following an algorithm similar to one put forward by Lafler & Kinman (1965). The period-finding program phases the data to a large sequence of test periods ranging between two user-specified periods. For each test period's phased data, the difference in differential magnitudes between adjacent points is summed. The sum of the magnitude differences is divided by the variance of the data

to indicate the goodness of the period. If my examination of the data phased to the test period finds that the lightcurve appears appropriately periodic, I rerun the program using a smaller period range with finer step sizes in order to zero in on the best period. I have recovered previously known periodic variables and refined their periods. I have also discovered six new periodic variables.

5.1.1 NGC 7789

In the Phase I data for NGC 7789 I recovered fourteen periodic variables previously found by Jahn, Kaluzny & Rucinski (1995) and Mochejska & Kaluzny (1999)(jointly: JKR/MK). I have also discovered two new binaries in the Phase I data and one more in the Phase II data.. Figure 5.1 is a color-magnitude diagram with the periodic variable stars marked. Table 5.1 lists the variables' properties cross-referenced to the work of JKR/MK. I have classified each eclipsing binary according to the criteria in the General Catalog of Variable Stars (Kholopov et al. 1985-1988, 1987, 1985, 1989; Kazarovets & Samus 1990; Kazarovets, Samus & Goranskij 1993; Kazarovets & Samus 1995, 1997; Kazarovets et al. 1999; Kazarovets, Samus & Durlevich 2000; Kazarovets et al. 1989). Each of the variables is discussed briefly below. The Phase I lightcurves are presented in Figure 5.2, and the Phase II multi-color lightcurve is shown in Figure 5.3.

JKR/MK found a total of fifty variable stars in the field of NGC 7789; I have recovered only fourteen of these due to the much smaller field of view ($23 \text{ arcmin} \times 23 \text{ arcmin}$ for JKR/MK vs. $14 \text{ arcmin} \times 14 \text{ arcmin}$ at MLO), but I have recovered all of the JKR/MK variables in the field. My analysis of stars 310, 413, 756, 1049, 1344, 1534, 2055, 2876, 2938, and 3214 agrees with that of JKR/MK in both period and type of variable star. All of these stars are eclipsing binaries, except the δ Scuti star, 3214.

Stars 3377, 3616, 3736, and 4277 were also examined by JKR/MK, but my analyses of these stars show some significant differences. For star 3377 (JKR/MK 2), I agree with their period and the classification of EW (W Ursae Majoris-type) in the paper by

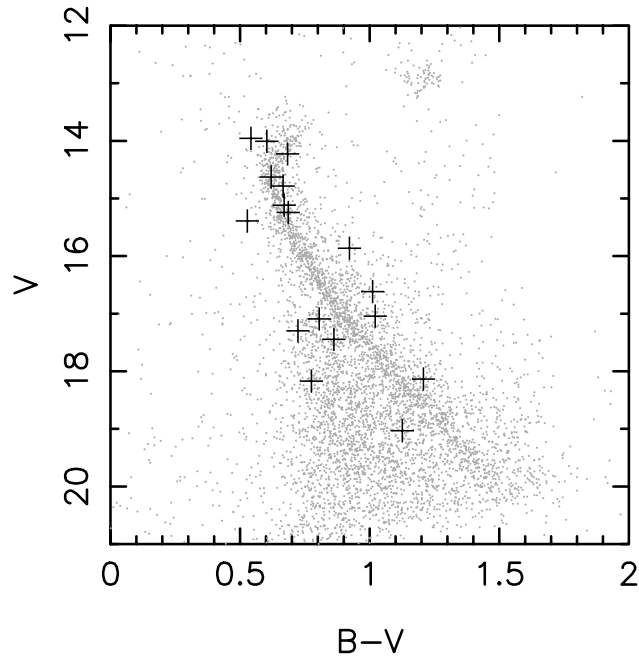


Figure 5.1: Color-magnitude diagram of NGC 7789 with periodic variable stars marked with crosses.

Star #	V	(B-V)	P(d)	JKR/MK	V_{max}	P(d)
310	18.106	1.207	0.37918	29	18.14	0.3791
413	16.982	0.805	0.30635	22	16.98	0.3063
756	18.039	0.775	0.48998	33	17.96	0.4902
1049	17.410	0.862	0.39559	31	17.36	0.3957
1344	17.291	0.723	0.70664	35	17.36	0.7061
1534	19.007	1.126	0.39083	9	19.13	0.7806
2055	14.232	0.683	1.17010	1	14.26	1.19
2741	14.013	0.603	0.18778
2840	17.054	1.021	2.3251
2876	15.859	-0.029	0.45780	7	15.93	0.455
2938	15.128	0.670	0.86054	8	15.19	0.85
3105	14.627	0.620	19.688
3214	13.969	0.542	0.08676	10	14.04	0.0955
3377	14.762	0.666	0.71790	2	14.81	0.72
3616	15.396	0.528	0.07835	15	15.47	...
3736	15.236	0.686	1.04802	3	15.30	0.70
4277	16.617	1.011	0.33783	4	16.72	0.337

Table 5.1: JKR/MK refers to papers by Jahn, Kaluzny & Rucinski (1995) and Mochejska & Kaluzny (1999). All stars except 2840 were recovered and verified in Phase I data and appear in Figure 5.2. Star 2840 was discovered in Phase II data and is shown in Figure 5.3.

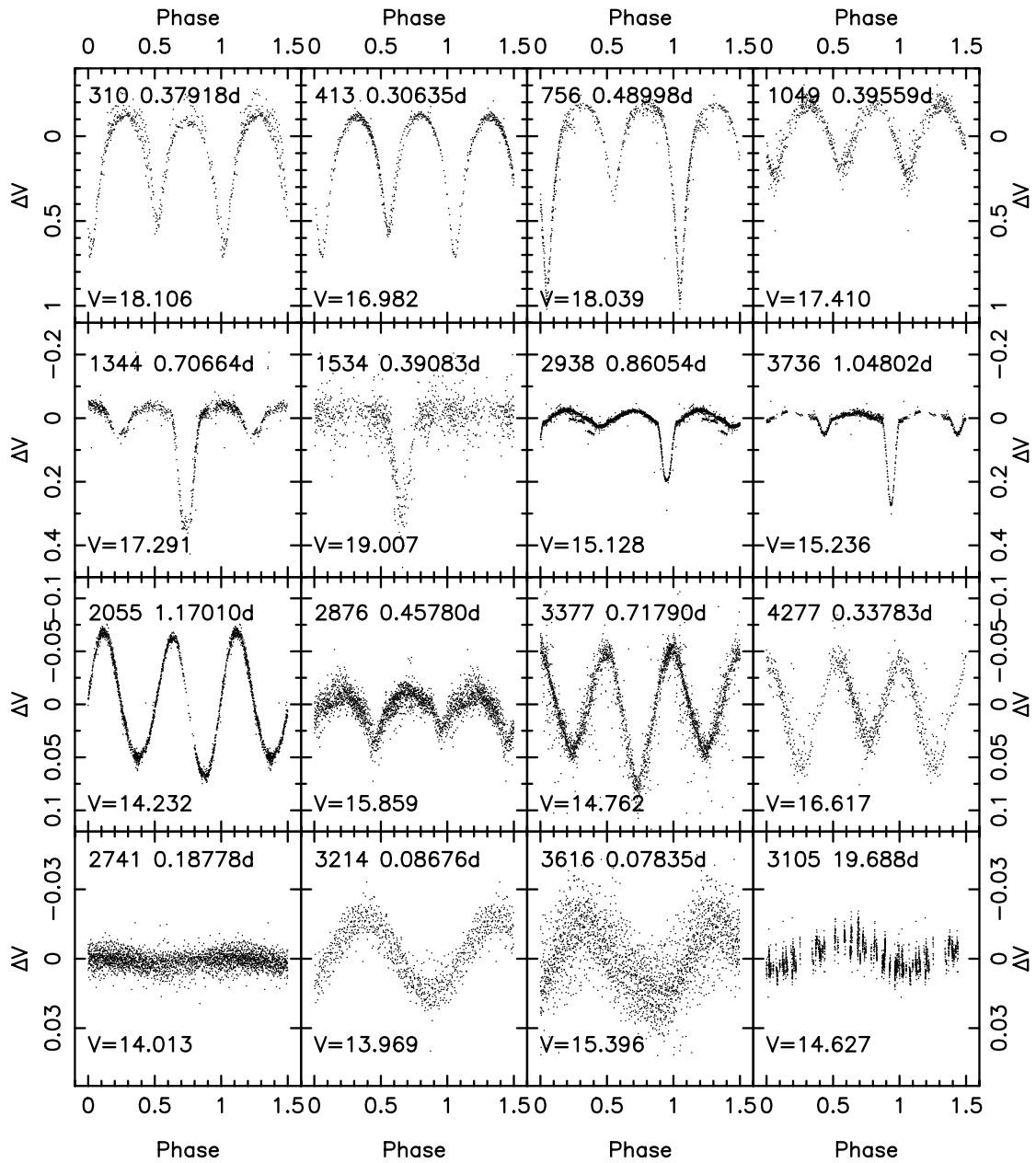


Figure 5.2: Periodic variable stars in NGC 7789. Note the differing scales on the Y-axis for each row.

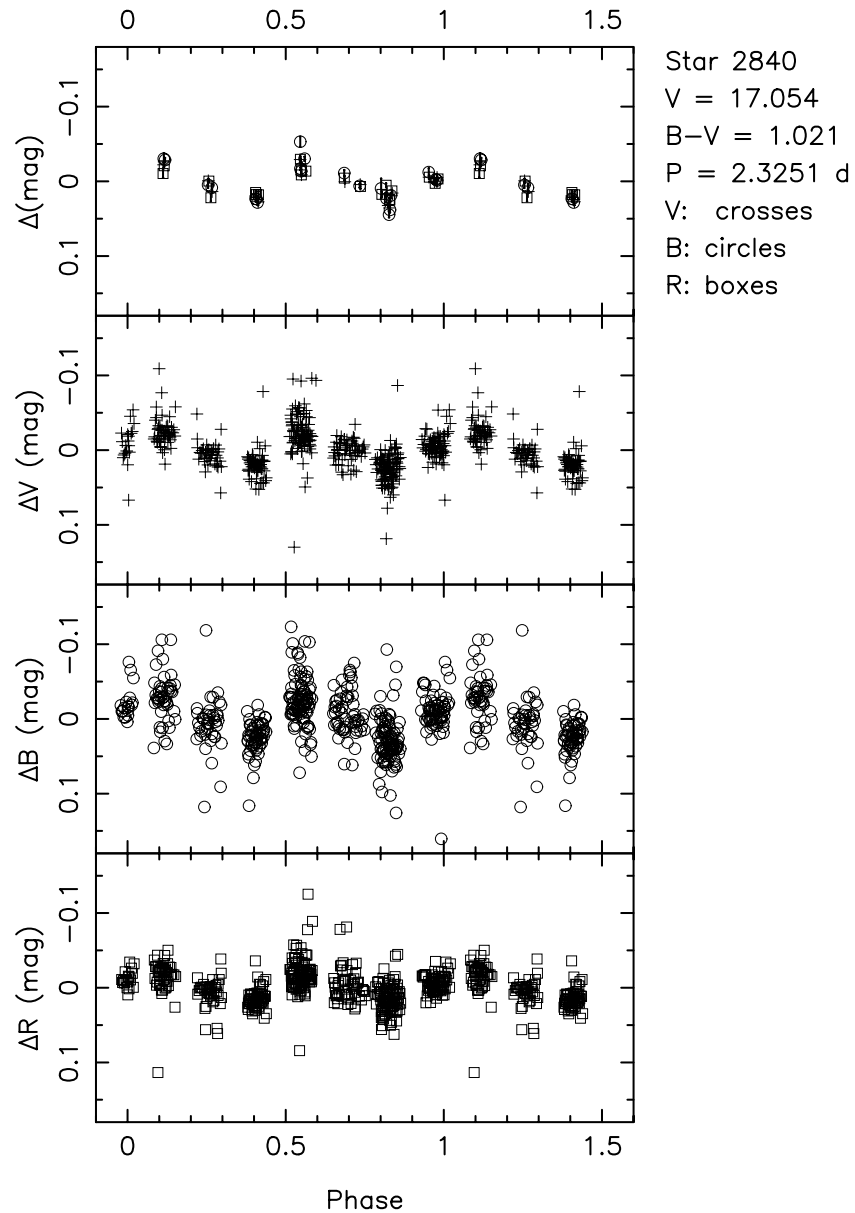


Figure 5.3: Periodic variable 2840 in NGC 7789. The top panel shows the BVR nightly mean magnitudes; the V data are crosses, the B are circles, and the R are boxes. Error bars are shown, but are generally smaller than the symbols. The lower three panels show the individual V, B, and R magnitudes measured on each frame. The x-axis is the phase of the lightcurve, using the period shown.

Jahn, Kaluzny & Rucinski (1995), but I do not agree with the later classification of EB (Beta Lyrae-type) in Mochejska and Kaluzny's paper (Mochejska & Kaluzny 1999). JKR/MK found no period for star 3616 (their 15), but believed it might be a δ Scuti; I have determined a period of 0.07835 d and agree with the δ Scuti designation. For star 3736 (JKR/MK 3), I significantly revise their period to 1.04802 d and classify this binary as EA (Algol-type). Finally, for star 4277 (JKR/MK 4), I agree with their period and classification, but the lightcurves look quite different - the maxima of the lightcurve presented here are approximately equal but the maxima in Mochejska & Kaluzny (1999) are unequal by ~ 0.05 mag.

I have discovered three previously unknown variable stars. Star 2741 has a period of 0.18778 d; it is likely a short period binary. Star 3105 was discovered via its power spectrum as described in § 3.3.3; it has a period of 19.688 d and was discussed in that section. Star 2840 was discovered in the Phase II data; it has a period of 2.3251 d. This star may be eclipsing, or the brightness variations may be due to some kind of reflection effect. The amplitudes of the lightcurves shown in Figure 5.3 decrease with wavelength, which indicates a thermal variation.

I have created finder charts for the new periodic variables. Figure 5.4 shows an image of NGC 7789 taken at the Mt. Laguna Observatory through the V filter on UT 1998 July 28. Smaller views as finder charts for the three new variables listed in Table 5.1 are marked and equatorial coordinates for the new variables are in Table 5.2. The smaller views are plotted in Figure 5.5.

5.1.2 NGC 6819

When I searched the Phase I NGC 6819 data for periodic variables, I recovered six previously known periodic variable stars from Street et al. (2002); I have refined their periods with the longer time baseline of the Phase I data. In the Phase II data, I found one new periodic variable. A CMD with the variable stars is in Figure 5.6. A table listing the

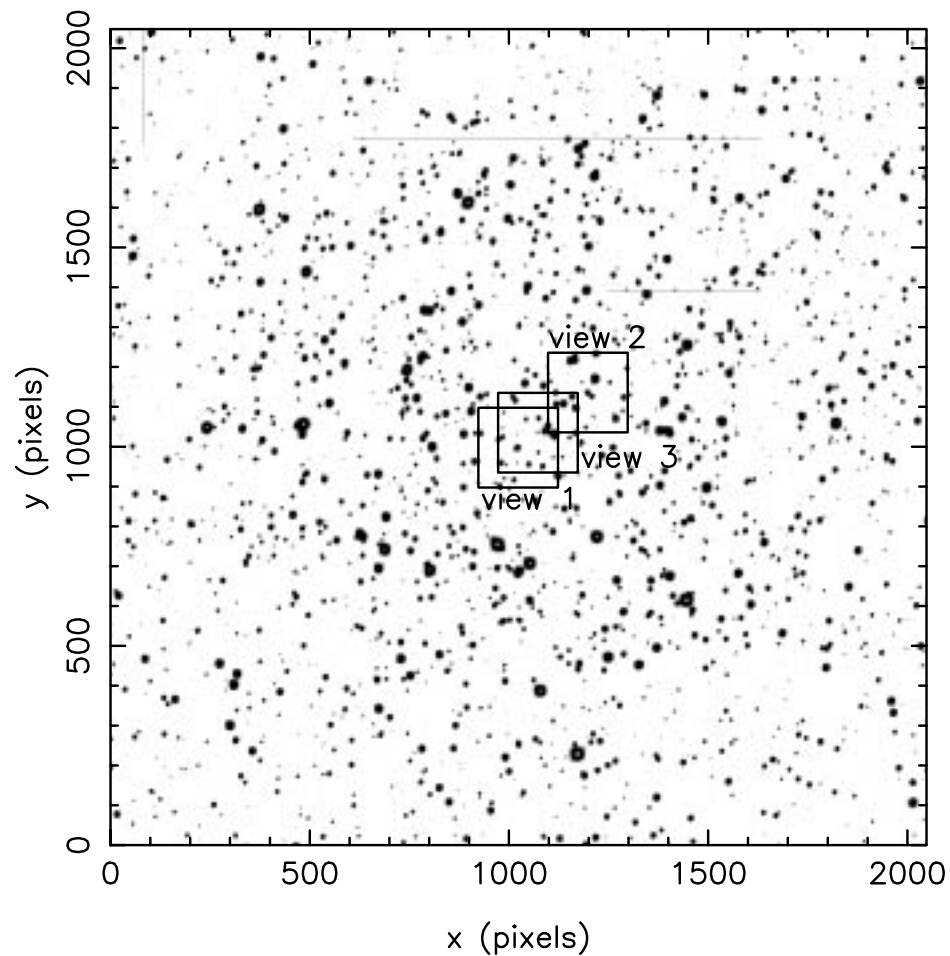


Figure 5.4: This image of NGC 7789 was taken at MLO and has a field of view of $14 \text{ arcmin} \times 14 \text{ arcmin}$. East is up and north is right. The smaller views marked on the image are shown in Figure 5.5.

Star #	V	RA (hms)	DEC (dms)
2741	14.013	23 57 22.10	+56 43 11.4
2840	17.054	23 57 23.94	+56 43 33.4
3105	14.627	23 57 28.58	+56 44 23.9

Table 5.2: Coordinates in the J2000 equinox for stars 2741 and 2840 were taken from the USNO-B1.0 catalog from the USNOFS Image and Catalogue Archive operated by the United States Naval Observatory, Flagstaff Station. Coordinates in the J2000 equinox for star 3105 were taken from the Hubble Guide Star Catalog, version 1.1, with a recalibration using the Astrographic Catalog/Tycho from the US Naval Observatory. Star 3105 is star GSC 4009-1286.

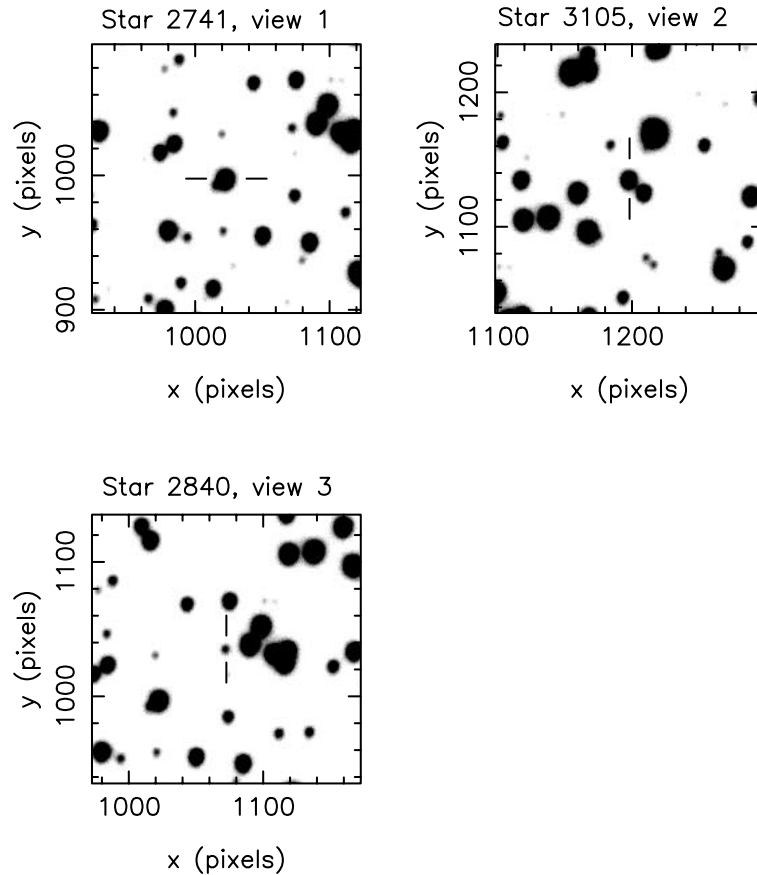


Figure 5.5: Finder charts for the new periodic variables listed in Table 5.1. East is up and north is right. The x , y coordinates are in pixels. Each pixel is approximately 0.41 arcsec. The celestial coordinates of each variable are listed in Table 5.2.

variables' properties and cross-referenced to the work of Street et al. (2002) is in Table 5.3.

The lightcurves of the five variables I recovered (589, 2926, 3004, 4244, 4291, and 4914) from the Phase I data are shown in Figure 5.7. Each lightcurve is in good agreement with those in Street et al. (2002), and I agree with the classification of EW for each binary.

Star 4187 was found in the Phase II BVR data. Its lightcurves are plotted in Figure 5.8; the top panel shows the nightly mean magnitudes in B, V, and R, while the lower panels show the individual magnitude measurements through each filter. From the color-magnitude diagram, star 4187 is a red giant. The period I determined is 17.6792 d. It is unclear from the lightcurves whether this is an eclipsing binary of some type or if the variability is caused by reflection or ellipticity effects. The J2000 coordinates for star 4187

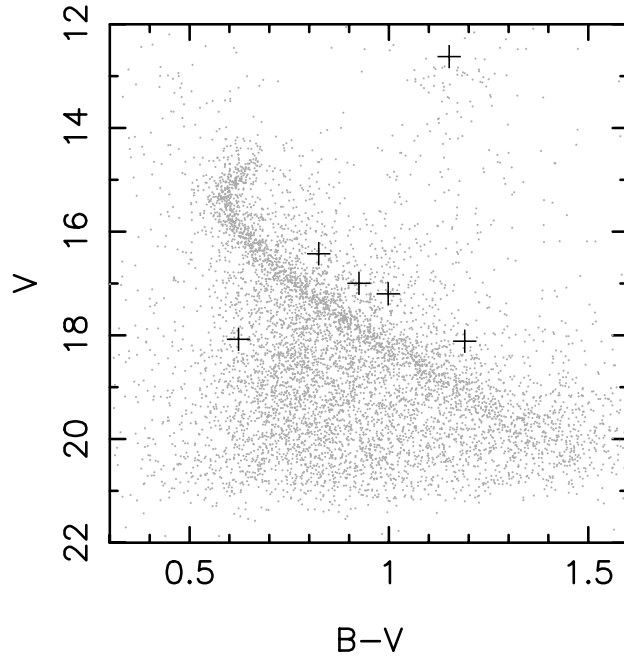


Figure 5.6: Color-magnitude diagram of NGC 6819 with periodic variable stars marked with crosses. Star properties are listed in Table 5.3.

Star #	V	(B-V)	P(d)	S#	V	P(d)
589	17.229	0.640	1.46884	7916	17.359	1.468
2926	16.427	0.824	0.36603	5834	16.610	0.3660
3004	18.078	0.623	0.33847	5660	18.172	0.3384
4187	12.624	1.151	17.6792
4244	17.201	0.998	0.30321	4448	17.494	0.3032
4291	18.114	1.190	0.25622	4441	18.275	0.2562
4914	16.998	0.925	0.35365	3856	17.246	0.293

Table 5.3: Properties of the periodic variables in NGC 6819. S# refers to the star number assigned in Street et al. (2002), and the subsequent two columns are taken from that paper.

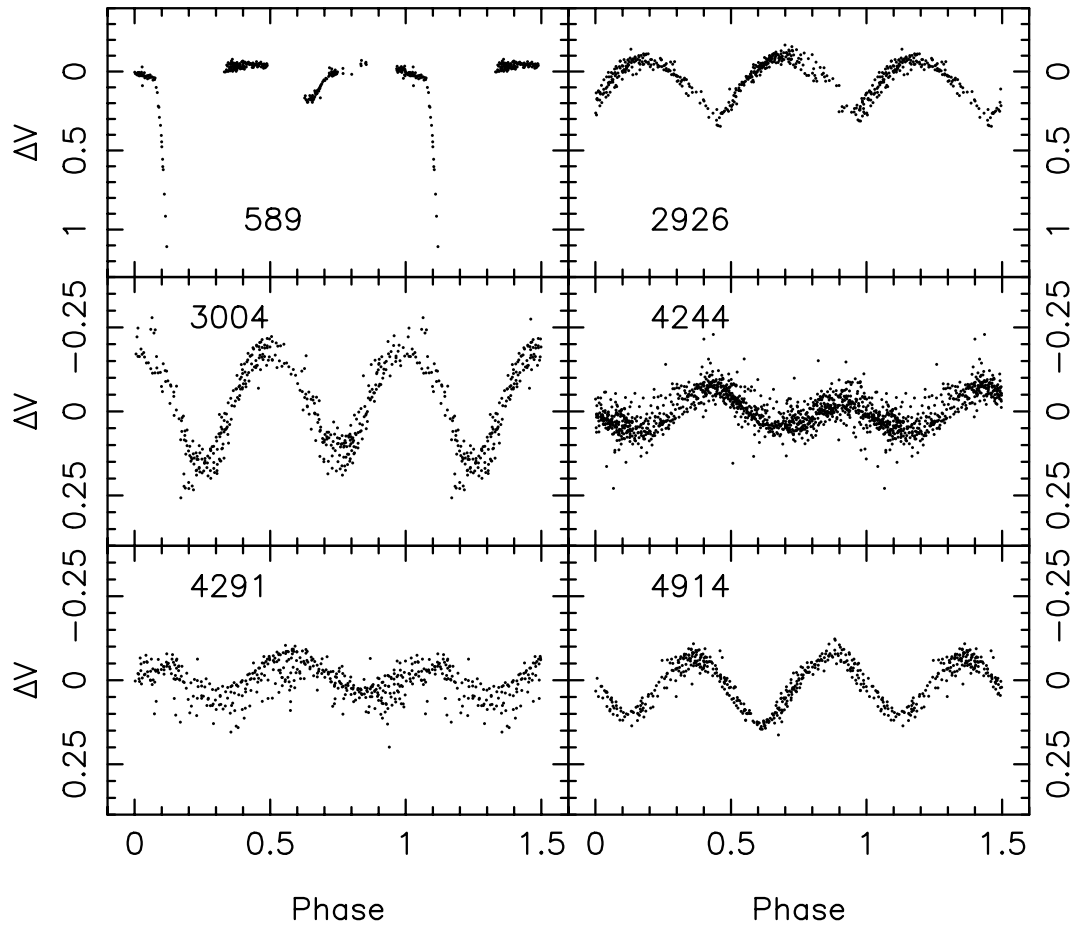


Figure 5.7: Periodic variable stars in NGC 6819. Note the different scales on the y-axes. Star properties are listed in Table 5.3.

are $RA = 19^h 41^m 21.89^s$ and $DEC = 40^\circ 12' 0.46''$, taken from the USNO-B1.0 catalog at the USNOFS Image and Catalogue Archive operated by the US Naval Observatory, Flagstaff Station. Figures 5.9 and 5.10 show images of NGC 6819 as finder charts.

5.1.3 M67

From the Phase I and Phase II data, I recovered one previously known variable star observed by Stassun et al. (2002). Star 5833, which is EV Cnc, has $V = 12.784$ and

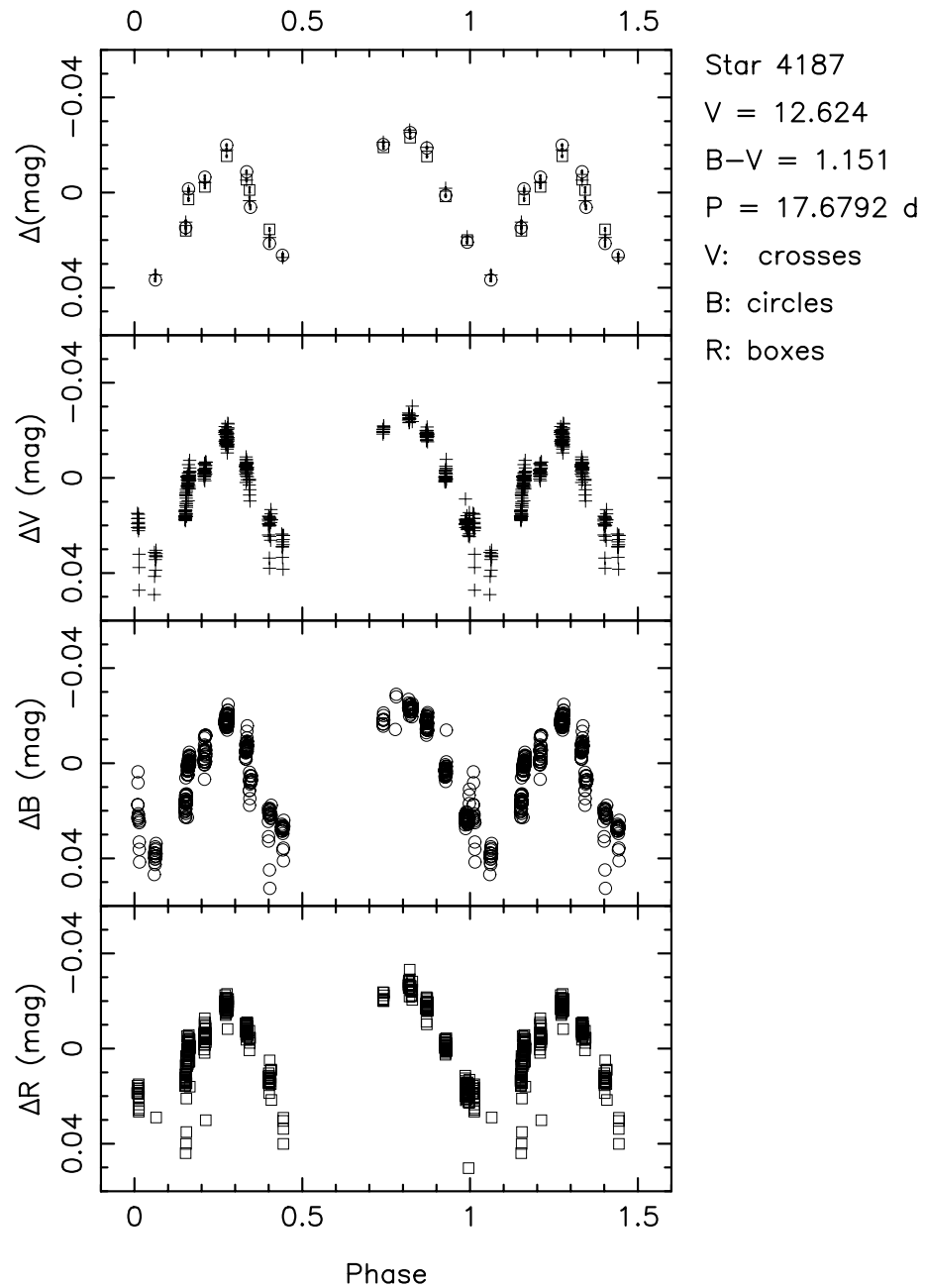


Figure 5.8: Periodic variable 4187 in NGC 6819. The top panel shows the nightly mean magnitude measurements: crosses are V, circles are B, and boxes are R. Error bars are shown on these measurements, but they are smaller than the symbols. The lower three panels show all of the V, B, and R magnitude measurements. The properties of star 4187 are listed in Table 5.3.

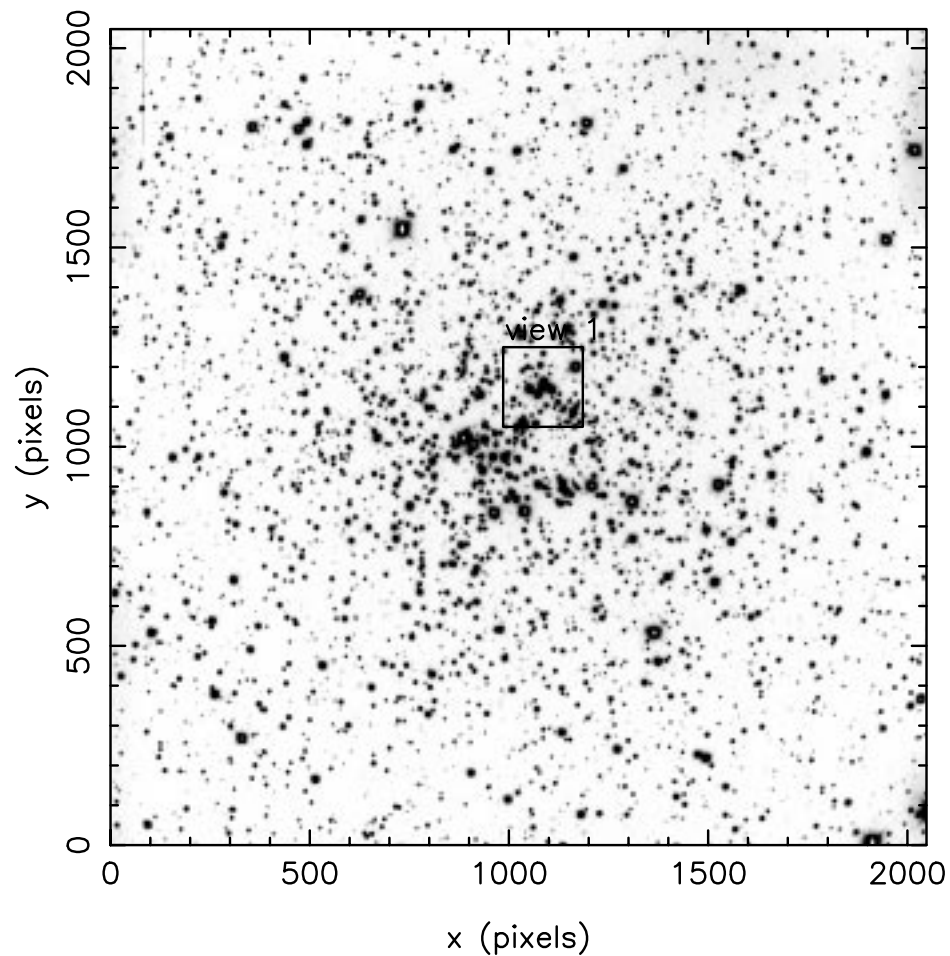


Figure 5.9: This image of NGC 6819 was taken at MLO and has a field of view of $14 \text{ arcmin} \times 14 \text{ arcmin}$. East is up and north is right. The smaller view marked on the image is shown in Figure 5.10.

$B - V = 0.487$ and corresponds to star 3706 in Stassun et al. (2002); a period of 0.44 d is listed. I have refined this period to 0.44144 d. Figure 5.11 shows the phased lightcurve for this variable. By referring to the CMD for M67 in Figure 3.33, panel a, one can see that this star is close to the main sequence turn-off.

5.1.4 NGC 188

In our Phase I data for NGC 188 I recovered two previously known variable stars observed by Kafka & Honeycutt (2003) (hereafter KH03) and discovered two new periodic variables.

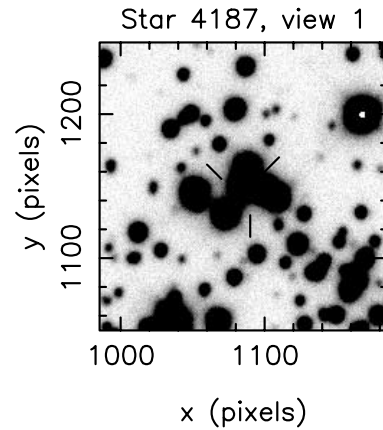


Figure 5.10: Finder chart for the new periodic variable in NGC 6819 listed in Table 5.3. East is up and north is right. The x, y coordinates are in pixels. Each pixel is approximately 0.41 arcsec. The celestial coordinates of the star are listed in the text.

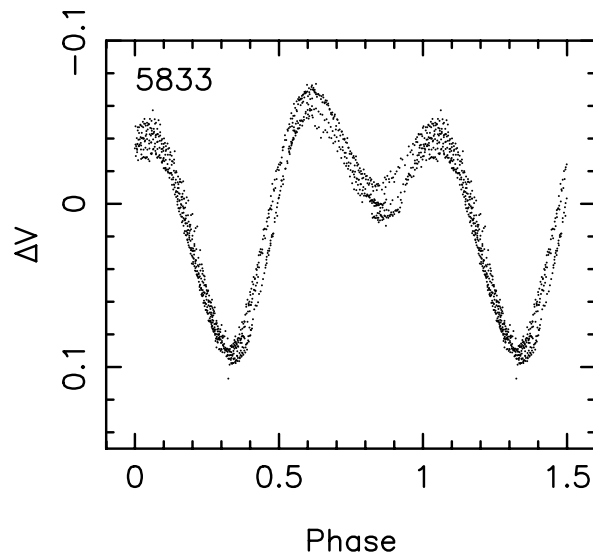


Figure 5.11: Period variable 5833 (EV Cnc) in M67. This star has $V = 12.784$ and $B - V = 0.487$.

In the Phase II data, I recovered two variables originally discovered by Kaluzny & Shara (1987), one of which was re-observed by Zhang et al. (2002) (jointly: KS/Z). The variables are shown in a CMD in Figure 5.12. A table listing the variables' properties and cross-referenced to the work of KH03 and KS/Z is in Table 5.4. I discuss the variables briefly

Star #	V	(B-V)	P(d)	Reference	Ref. #	V/I	P(d)
382	15.820	0.856	0.28574	KH03	WV11	16.0 (V)	0.28574
621	16.211	0.961	0.5859	KS/Z	v5	15.49 (I)	0.585984
707	16.738	0.832	0.30690	KH03	WV14	16.8 (V)	0.30797
742	16.188	0.816	0.3304	KS/Z	v6	15.68 (I)	0.3305
873	16.352	0.841	0.32819
1206	15.324	0.958	2.09381

Table 5.4: NGC 188 Periodic Variables' Properties. The references are: KH03 is Kafka & Honeycutt (2003), and KS/Z refers jointly to Kaluzny & Shara (1987) and Zhang et al. (2002). The subsequent columns refer to data from those sources.

below. The lightcurves are presented in Figure 5.13.

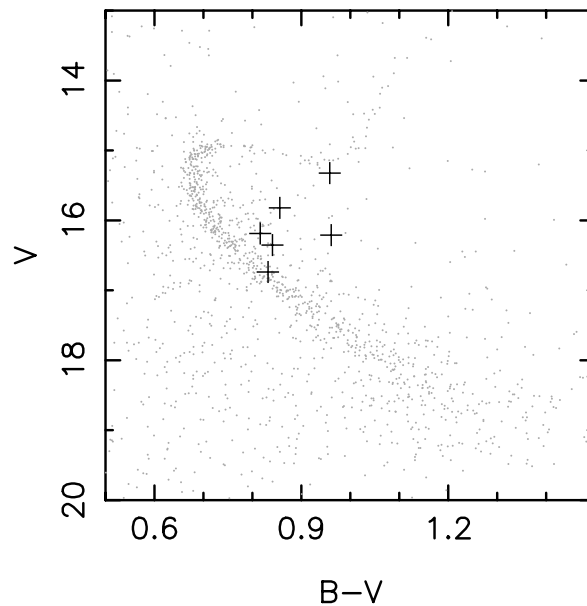


Figure 5.12: Color-magnitude diagram of NGC 188 with periodic variable stars marked with crosses.

For the previously-known variables, I use the most recent labels, magnitudes and periods. KH03 found periods for thirty-five variable stars in the field of NGC 188; I have recovered only two of these due to the much smaller field of view ($17 \text{ arcmin} \times 17 \text{ arcmin}$ vs. the 14 arcmin field at MLO and $3 - 5 \text{ arcmin}$ field at the Perkins). As KH03 indicates,

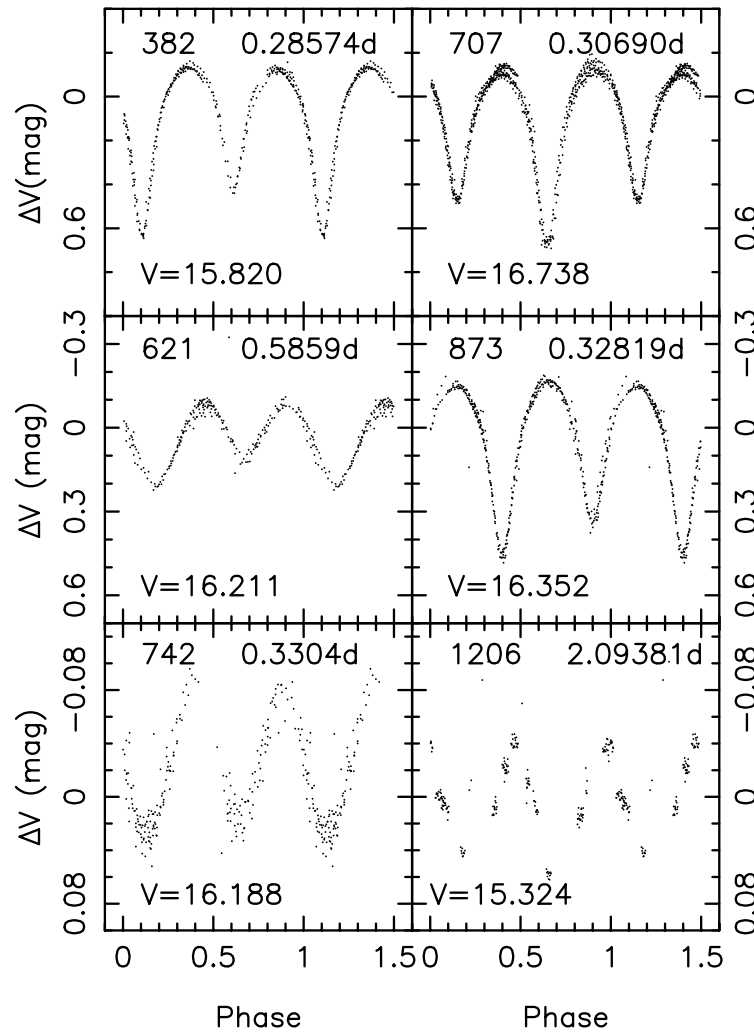


Figure 5.13: Periodic variable stars in NGC 188. Note the different scales on the y-axes.

the two variables I recovered had been discovered by Zhang et al. (2002). Our analysis of stars 382 and 707 agrees with the previous determination that these stars are likely W Ursae Majoris binaries. The period determined here for star 382 is a perfect match to the period in KH03. The period for star 707 is slightly shorter than that in KH03.

Star 621 was originally observed by Kaluzny & Shara (1987) and re-observed by Zhang et al. (2002). The period and lightcurve here agree very well to those of KS/Z. Star 742 was also originally observed by Kaluzny & Shara (1987), but Zhang et al. (2002) were unable to refine the period due to photometric noise. The period I determined agrees well

with that originally found by Kaluzny & Shara (1987).

The lightcurve for the new periodic variable, star 873, is very similar to the previous periodic variables discussed above; it is also a likely W Ursae Majoris binary. Its period of 0.32819 d is typical for a binary of this type. From the reference star file from Sarajedini (2003), this binary is located at RA= $0^h 46^m 14.8s$ and DEC= $85^\circ 13' 56.1''$, in 2000 coordinates. Finder charts for this star is located in Figures 5.14 and 5.15.

I also discovered the periodicity of star 1206 in the Phase I data. Although its lightcurve is much sparser than the others, it also appears to be a W Ursae Majoris binary. Sarajedini (2003) list the J2000 coordinates for this star as RA= $0^h 42^m 44.2s$ and DEC= $85^\circ 16' 46.2''$. Figures 5.14 and 5.15 also give finder charts for 1206.

5.2 Binary Sequences

Binary stars may show higher levels of stellar activity (e.g., Schijver & Zwaan (1991)). The tidal locking of the components of binary stars and the effect of this on each star's rotation period could have an effect on the photospheric activity of the star. In order to explore this possibility, I have selected stars falling on the binary sequence within each cluster. If the typical binary star has components of equal mass, then the brightness of the binary will be twice that of each component; consequently the binary sequence will fall 0.75 mag above the main sequence. Using the center of the photometric main sequence determined in the Phase I analysis, I chose stars falling 0.75 mag above the main sequence and assumed the binary sequence width in color was about 0.1 mag. In this section I will discuss the activity of stars falling on the binary sequence in the Phase II data. Figure 5.16 shows the binary sequences on the color-magnitude diagrams for each cluster. The Phase II data only contained a fraction of the binary stars because of the small field of view.

I followed the same analysis procedure as in Chapter 4 for the main sequence stars. I calculated the significance indices, activity indices and the errors in the activity indices for the binary stars, only including those binaries with at least five nights of observations in V.

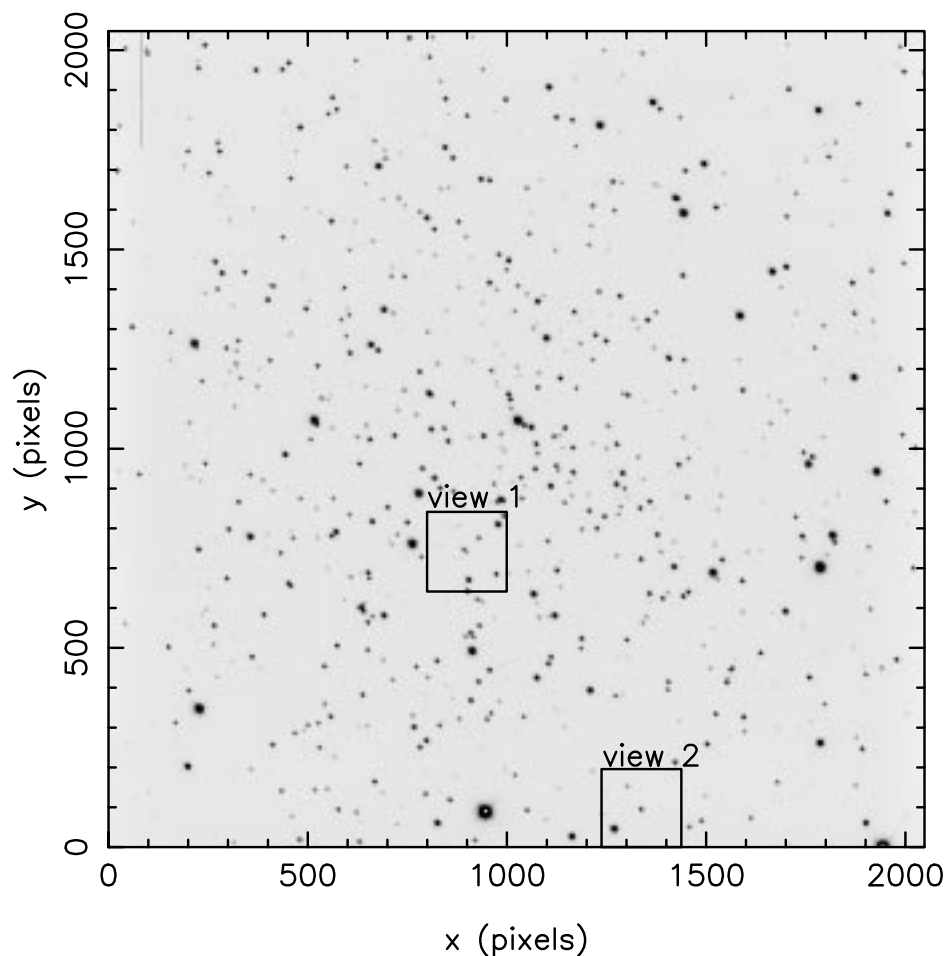


Figure 5.14: This image of NGC 188 was taken at MLO in July 1998 and has a field of view of $14 \text{ arcmin} \times 14 \text{ arcmin}$. East is up and north is right. The smaller views marked on the image are shown in Figure 5.15.

Then I calculated the correlation coefficient for the nights with observations through BV and/or VR filters. Those stars with $\alpha_v \geq 3$ and positively correlated at a 99% significance level are the active binaries. However, since the small field of view limited the number of binaries observed, only a few are active. Table 5.5 summarizes the results of this analysis. The percentage of active binaries is similar to the percentage of active main sequence stars; however, the actual number of active binary stars is very small.

How does the behavior of the entire observed binary sequence compare to that of the main sequence? Figure 5.17 shows the mean V differential magnitudes for each night

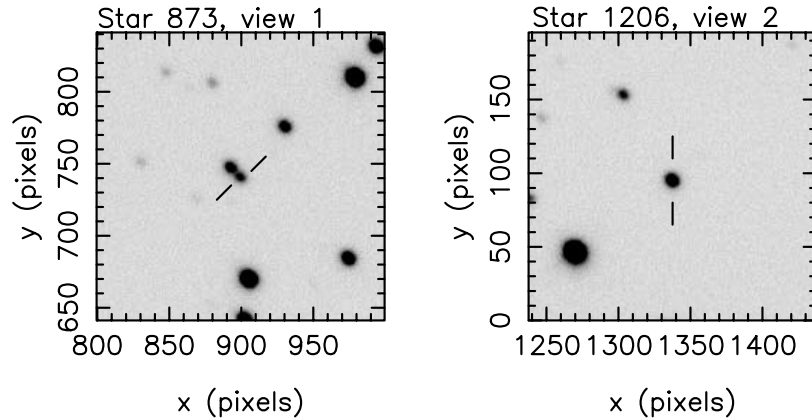


Figure 5.15: Finder charts for the new periodic variables discussed in the text. East is up and north is right. The x , y coordinates are in pixels. Each pixel is approximately 0.41 arcsec. The celestial coordinates for the stars are listed in the text.

versus the mean B and R differential magnitudes on the same nights; the left column of panels shows the main sequence stars in each cluster and the right column of panels show the binary stars. The lines were fit using the least squares method, and the slopes of the lines can be found in Table 5.6. The ΔV vs. ΔB and ΔR plots of the binary stars look very similar to the plots of the main sequence stars. The slopes of the main sequence stars and binary stars in NGC 7789 are essentially the same, which is also the case for NGC 6819.

The binary sequence populations in the four clusters show no sign of higher levels of activity than the main sequence stars; the binaries in this analysis either do not have enhanced activity from the spin-up of the rotation of the individual stars, or the few binaries observed are wide systems that would not have the spin-up effect. The fraction of active stars on the binary sequence is similar to the fraction of active stars on the main sequence. However, it should be noted that there are only one or two active binaries in each cluster; the small number of active stars may be biasing the result.

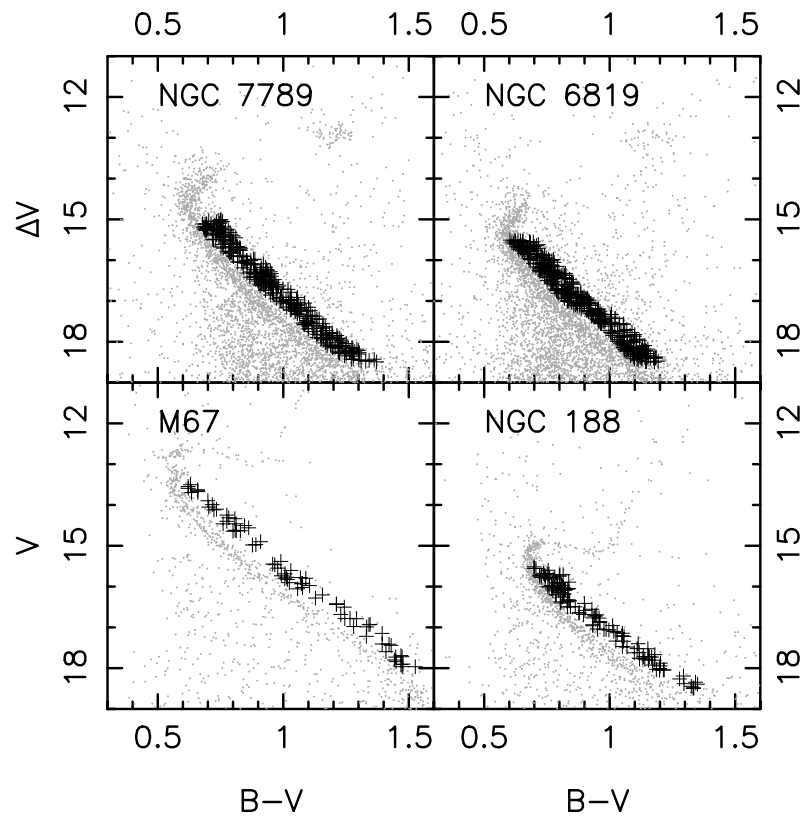


Figure 5.16: Color-magnitude diagram showing the binary sequence of each cluster. The gray dots are all stars observed, and the crosses are the stars which are chosen to be on the binary sequence.

Cluster	σ_{ens}	# Bin.	# Cand. Var.	# Bin.	# 99% sig.	# Active	Active MS
NGC 7789	2.5	16	4 (25%)	16	10 (65%)	1 ± 1 (6%)	12%
NGC 6819	1.5	35	1 (3%)	35	20 (57%)	1 ± 1 (3%)	4%
M67	2.0	6	3 (50%)	7	6 (86%)	2 ± 1 (33%)	28%
NGC 188	1.5	9	1 (11%)	9	4 (44%)	0	0%

Table 5.5: Summary of Binary Sequence Activity. The second column lists the ensemble error in millimagnitudes that was determined from the plots of σ_{mean} and σ_{rms} and applied to the binary sequence analysis. The third column lists the number of binary sequence stars with at least five nights of observations in V that were included in the activity index calculation. The fourth column is the number of candidate variable binary stars found. The fifth column is the number of binary sequence stars with at least five pairs of B and V and/or V and R observations on the same night; these stars were included in the correlation coefficient calculation. The sixth column is the number of binaries whose correlation coefficients were 99% significant. The seventh column listing the fraction of active stars uses the lower of the two binary sequence star numbers. The last column lists the percentage of active stars found in the main sequence population of each cluster.

Cluster	Population	Slope	χ^2_ν	# Points
NGC 7789	main seq.	0.59 ± 0.01	64	4965
NGC 7789	binary seq.	0.55 ± 0.03	92	565
NGC 6819	main seq.	0.46 ± 0.01	130	7145
NGC 6819	binary seq.	0.46 ± 0.02	250	981
M67	main seq.	0.94 ± 0.02	280	1881
M67	binary seq.	0.42 ± 0.04	220	197
NGC 188	main seq.	0.39 ± 0.02	65	2140
NGC 188	binary seq.	0.55 ± 0.05	100	268

Table 5.6: Results of the line fits to the data in Figure 5.17 for all clusters studied. The lines were fit according to the least squares method. The last column is the number of data points plotted in each panel of the figure.

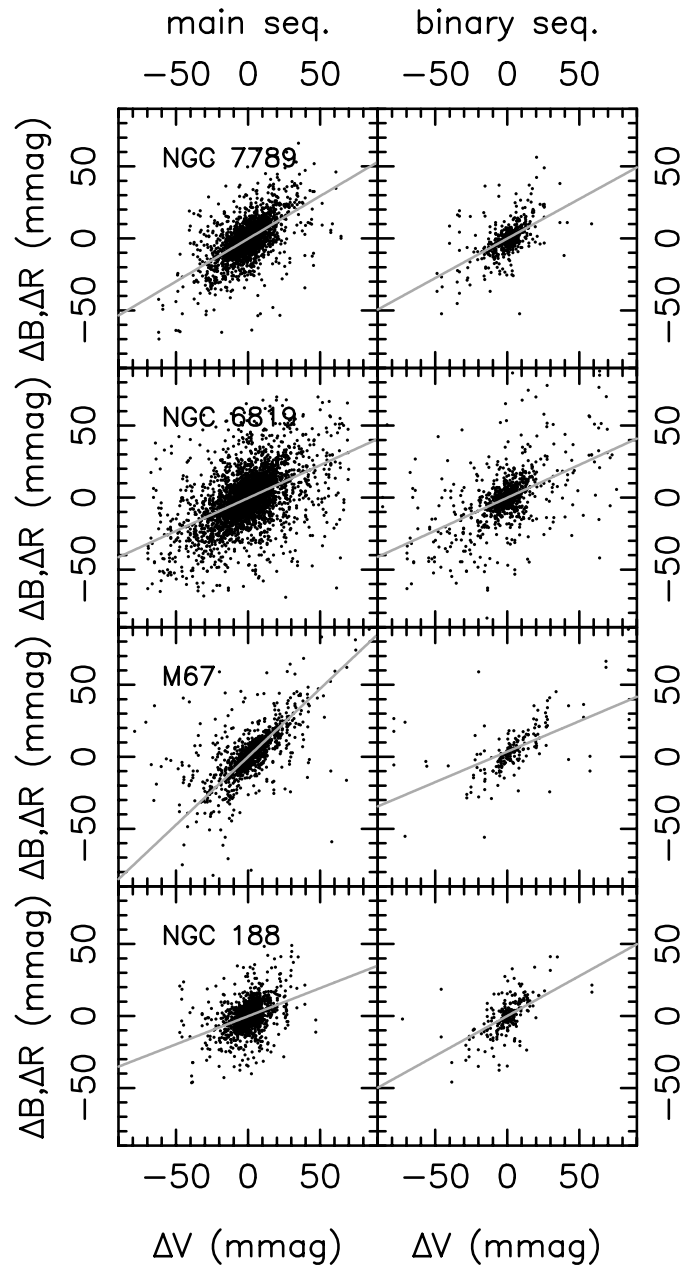


Figure 5.17: Mean V differential magnitudes versus mean B or R differential magnitudes for the main sequence stars in all the clusters in the left column. The right column of panels shows the same for the binary sequence stars. The slopes of the lines can be found in Table 5.6.